EFFICIENT DESIGN OPTIMIZATION OF A THERMOELECTRIC GENERATOR BY A COMBINATION OF MODEL ORDER REDUCTION AND THERMAL SUBMODELING TECHNIQUES

Chengdong Yuan[1,2], Gunasheela Sadashivaiah[2], Tamara Bechtold[1,2]
[1]Jade University of Applied Sciences
Department of Engineering
Friedrich-Paffrath Str. 101, Wilhelmshaven, D-26389, Germany
[2]University of Rostock
Institute for Electronic Appliances and Circuits
Albert-Einstein Str.2, Rostock, D-18059, Germany
E-Mail: {chengdong.yuan, tamara.bechtold}@jade-hs.de, gunasheela.sadashivaiah@uni-rostock.de

Evgenii B. Rudnyi
CADFEM GmbH
Marktplatz 2, Munich, D-85567
Grafing near München, Germany
E-mail: erudnyi@cadfem.de

KEYWORDS
Energy harvesting, Human body tissue simulation, Model order reduction, Submodeling.

ABSTRACT

The aging European population leads to the important role of electrically active medical implants for medical therapies. Combined with energy harvesting technology, the power supply life time of the medical implants can be extended. In this work, we introduce a miniaturized thermoelectric generator (TEG), which transforms the thermal energy into electrical energy, embedded in a realistic human forearm model. For efficient design optimization of TEG, we present a combination of model order reduction (MOR) and thermal submodeling methodology. The representative TEG positioned global thermal human forearm model is first reduced to a compact size through MOR method. Secondly, the temperature results from the reduced model are projected back to the full-scale and used as the boundary conditions for the detailed TEG submodel.

INTRODUCTION

The increasingly aging population of Europe will be a large problem in the next few decades. This trend leads to the importance and necessity of developing implants for medical therapies, such as bone and cartilage regeneration and deep brain simulation to treat movement disorders. However, one of the main drawbacks of such medical implants is their limited battery life.

Energy harvesting technologies are widely developed nowadays as an efficient solution for self-powered implantable medical devices, which have improved the implants' lifetime (Amar et al 2015). In this paper, a thermoelectric generater (TEG) would be introduced, which transforms the themal energy in the human body into electrical energy through the Seebeck effect.

As suggested from the previous research (Yang et al 2007, Jadhav et al 2017), the TEG is positioned in the fat layer, where the highest temperature difference occurs. In these research projects, simplified human tissue cube model was proposed for the simulation of human tissue. In addition, the authors (Jadhav et al 2017) applied a Krylov-subspace based model order reduction (MOR) technology to a linear thermal model. This was then exposed to constant heat generation input in the muscle layer and convection effect at the skin surface. An accurate and compact reduced order model was generated for the fast simulation of temperature distribution results on TEG.

In the present work, a newly designed TEG would be embedded into a realistic human left-hand forearm model adopted from Verma (Verma et al 2018). Instead of using constant metabolic heat generation as the heat input, the bio-heat model of the human tissue (Pennes 1948) would consider the blood perfusion, metabolic heat generation rates in different tissue layers and the convection effect at the skin surface. The blood perfusion heat generation results in temperature-depended nonlinear inputs in the system. For the application of conventional MOR algorithms (Freund 2000, Antoulas 2005), which are designed for linear systems, a linearization strategy is suggested for the bio-heat thermal system in this paper. Furthermore, to do the design optimization of the TEG, a submodeling technique is implemented, which separates the simulation of the thermal human tissue model and the multiphysics domain TEG model.

STUDY CASE

The simulations are carried out in software ANSYS® Mechanical based on a realistic 3D human left-hand forearm model with a disc-shaped TEG device embedded

inside. Blood perfusion and metabolic heat generation rates are considered in the layers of muscle, fat and skin tissue. The convection effect at the skin surface is used as the boundary condition.

Human Left-hand Forearm Model

Adapted Verma's model (Verma et al 2018), a human left-hand forearm model is applied for the temperature distribution simulation of human tissue (see Figure 1). The model is constructed with layers of muscle, fat, skin, and with blood vessels and bones. The material properties of each human tissue are shown in Table 1.
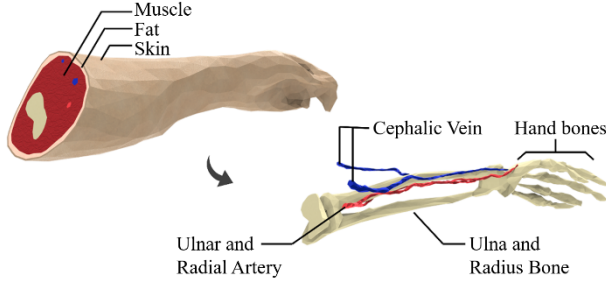

Figure 1: Human forearm model with bones and blood vessels adapted from (Verma 2018)

Table 1: Material properties of various tissue types

Tissue type	Density	Specific heat	Blood perfusion rates	Metabolic heat rates
	ρ (kg/m^3)	c (J/kgK)	ω (1/s)	Q_m (W/m^3)
Muscle	1090.4	3421.2	3.37×10^{-4}	498.52
Fat	911	2348.3	3.01×10^{-4}	279.8
Skin	1109	3390.5	9.06×10^{-4}	841.57
Blood	1049.8	3617		
Bone	1908	1312.8		

After the spatial discretization with finite element method (FEM) in ANSYS® Mechanical, the human forearm model could be presented by the bio-heat equation (Pennes 1948), where the temperature-depended non-linear blood perfusion and constant metabolic heat generation rates in different human tissues are accounted for the heat sources. The system equations of the forearm model reads as follows:

$$\Sigma_N \begin{cases} E \cdot \dot{T}(t) + A \cdot T(t) = \underbrace{B \cdot u(T(t))}_{Q} \\ y(t) = C \cdot T(t) \end{cases} \quad (1)$$

where $A, E \in R^{N\times N}$ are the global heat conductivity and heat capacity matrices, $B \in R^{N\times m}$ is the input distribution array and $C \in R^{q\times N}$ is the output matrix. $T(t) \in R^N$ is the vector of the unknown temperatures, N is the dimension of the system and m, q are the number of inputs and user-defined outputs, respectively. The load vector Q is given as:

$$Q = \underbrace{\rho_b c_b \omega(T_a - T(r,t))}_{Q_p} + Q_m \quad (2)$$

where ρ_b, c_b are the blood's density and specific heat and ω is the perfusion rate of the tissue. $T_a = 37°C$ is the arterial blood temperature and $T(r,t)$ is the resulting temperature distribution in the perfused tissues. In this forearm model, blood perfusion heat generation rate Q_p and metabolic heat generation rate Q_m are applied in muscle, fat and skin tissue layers. In addition, the heat dissipated from the skin surface is modelled by convection boundary condition:

$$q_\perp = h \cdot (T(t) - T_{amb}) \quad (3)$$

where $q_\perp$ is the heat flux normal to the boundary skin surface, T_{amb} is the ambient temperature and h is the heat transfer coefficient in W/m^{2}K.

Thermoelectric Generator

Thermoelectric generators transform the thermal energy into electrical energy through the Seebeck effect of thermoelectric materials. In this paper, a TEG model with 16×16 thermocouple legs is presented (see Figure 2).
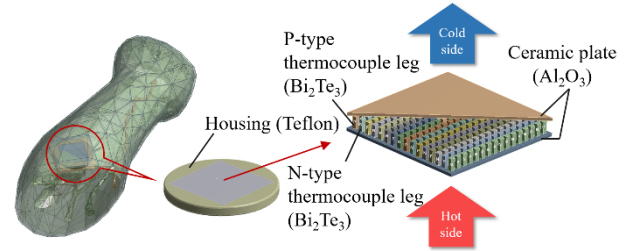

Figure 2: Thermoelectric generator positioned in fat layer in human left-hand model

Table 2: Material properties of various parts in TEG

TEG Parts	Material type	Density	Specific heat	Thermal conductivity
		kg/m^3	J/kgK	W/mK
Housing	Teflon	8933	385	0.25
Ceramic plates	Al$_2$O$_3$	3720	880	25
Couple legs (P-type)	Bi$_2$Te$_3$	7700	90	1.52~1.58
Couple legs (N-type)	Bi$_2$Te$_3$	7700	90	1.58~1.62

The TEG model contains two ceramic plates (24.64mm×24.64mm×0.565mm) with 16×16 P-type and

N-type Bismuth Telluride made thermocouple legs (0.8mm×0.8mm×2.27mm) in between. The TEG is further protected by a cylindrical Teflon housing (radius 19mm). The material properties of this TEG are presented in Table 2, where the thermal conductivity of the thermocouple legs are temperature-depended.

It is further placed in high-fat regions as suggested through the steady-state thermal simulation of forearm model. The maximum temperature difference is observed in the fat tissue layer (see Figure 3).
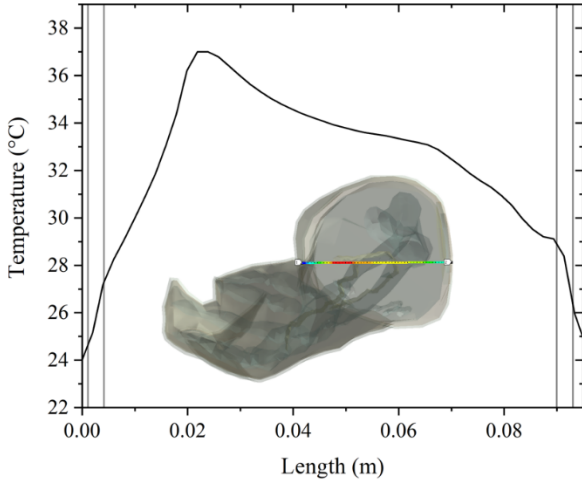

Figure 3: Temperature distribution profile along the cut side of the human forearm model

According to Seebeck effect, the temperature difference between hot and cold sides of the TEG plates will be transferred into electrical energy through the thermocouple legs. The hot side of TEG is near to the artery where temperature is maintained at $37°C$. In addition, through the convection effect at the skin surface, the heat dissipates and flows through the TEG device from hot to cold side. A Seebeck voltage output could be generated from the TEG through the equation, which is directly proportional to temperature difference:

$$V_{out} = n \cdot \Delta T(\alpha_1 - \alpha_2) \qquad (4)$$

where n presents the number of thermocouple legs, ΔT is the temperature difference between the top and bottom surfaces of the thermcouple legs and α_1, α_2 are the Seebeck coefficients.

A COMBINATION OF MODEL ORDER REDUCTION AND SUBMODELING

The simulation of the human forearm model with an embedded detailed TEG model spends a large computational effort due to its large dimensional FEM model. The detailed TEG positioned forearm model shown in Figure 2 has a total 233,857 DoF (127,307 DoF from the detailed TEG, 106,550 DoF from the forearm tissue). During the design optimization process, the geometry modifications of the TEG will lead to the repeat simulations of the whole model. In order to improve the

computational efficiency, submodeling and model order reuduction techniques are combined and used.

Submodeling Technique

Submodeling technique separates the simulation of thermal human tissue model and coupled-domain TEG model. Firstly, a representative TEG model is positioned within the thermal human forearm model. In this representative TEG model, the structure of the thermocouple legs are replaced by block structure instead, which has less degrees of freedom after the spatially discretization. The material properties of the block structure are used based on the experimental data (Yalkoti 2017), where the thermal conductivity is calculated as linear. This leads to the system matrices in equation (1) all linear. The thermal simulation of the representative TEG positioned human forearm model is processed and its distribution temperature results are further used as the boundary conditions for the detailed TEG submodel (see Figure 4).
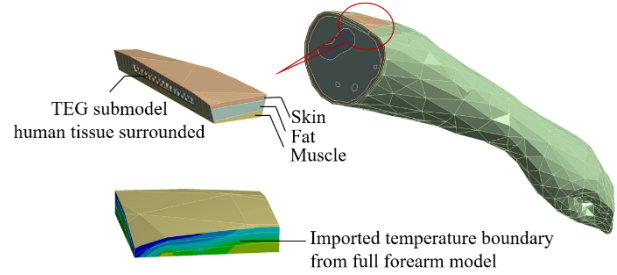

Figure 4: Detailed TEG submodel with surrounding human tissue. Temperature results from the global full forearm model are imported as the temperature boundary conditions in the submodel

In order to minimize the influence of the human tissue on the TEG model, the TEG submodel is surrounded with a small part of human tissue. In this way, the detailed TEG submodel simulation is separated from the global forearm model. One could change the structure of the TEG model and do the repeat simulations in the submodel only.

Model Order Reduction

Although the submodeling technique avoids the repeat thermal simulations of the global forearm tissue model, one still need one full-time simulation of the large-scale forearm model (109,244 DoF) to get the temerpature results as the temperature boundary conditions for the submodel. To have a fast simulation of the full forearm linear thermal model, mathematical model order reduction (MOR) algorithm has proved its robustness (Bechtold et al 2013). This technique generates highly accurate and compact model which enables a fast simulation of the forearm tissue model.

Based on FEM, the forearm thermal model is presented by equation (1) and (2). The blood perfusion heat generation rate is temperature-depended, which leads to

a non-linear input, whereas all other system matrices are constant. According to this property, the temperature-depended part could be transferred to the left-hand side and integrated in the global heat conductivity matrix:

$$\sum_N \begin{cases} E \cdot \dot{T}(t) + (A + \rho_b c_b \omega \cdot I) \cdot T(t) = \rho_b c_b \omega T_a + Q_m \\ y(t) = C \cdot T(t) \end{cases}$$

$$(5)$$

where $I \in R^{N \times N}$ would be a unity matrix if perfusion would take place in all volumes of the model. In our implementation, the blood perfusion heat generation rate is treated as a 'convection-type' effect due to the analogy between Q_p and $q_\perp$. In ANSYS® Mechanical, element type LINK34 is created between each node in the forearm tissue model and the user defined external arterial temperature node. The perfusion heat generation rate in equation (2) will then be treated as a convection boundary condition on each node. The film coefficient h in this special convection boundary condition is analogy to the blood perfusion rate coefficient $\rho_b c_b \omega$, which is set as negative. This means that the heat flows into the human tissue and this effect is equivalent to heat generation input (see Figure 5).
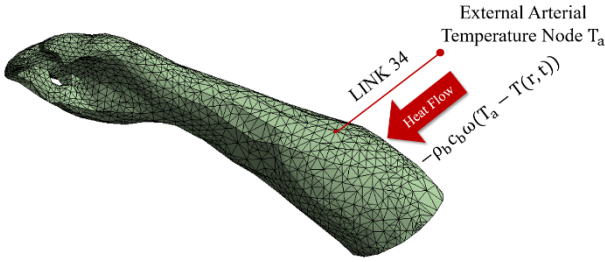

Figure 5: Blood perfusion heat generation defined as "Convection-type" in ANSYS® Mechnical

Therefore, this newly obtained thermal system is now linear, which contains only the constant metabolic heat generation rate Q_m on the right-hand side. With this linearized model, the conventional Krylov-subspace based MOR is applied to obtain a reduced system. In this case, software ModelReduction inside ANSYS (Rudnyi and Korvink 2006) is used:

$$\sum_r \begin{cases} \underbrace{V^T E V}_{E_r} \cdot \dot{z}(t) + \underbrace{V^T \tilde{A} V}_{A_r} \cdot z(t) = \underbrace{V^T \cdot Q_m}_{Q_r} \\ y(t) = \underbrace{C V}_{C_r} \cdot z(t) \end{cases}$$

$$(6)$$

where $V \in R^{N \times r}$ is the reduced order projection matrix generated based on the Krylov-subspace $\mathcal{K}_r\{-\tilde{A}^{-1}E, -\tilde{A}^{-1}Q_m\}$ around the expansion point $s_0 = 0$ Hz. $E_r, A_r \in R^{r \times r}$ are the reduced system matrices, where A_r is reduced from the blood perfusion heat integrated conductivity matrix $\tilde{A}$ through the application of element LINK34 in ANSYS® Mechanical. $Q_r \in R^r, C_r \in R^{q \times r}$ are the reduced metabolic heat generation load vector and output matrix respectively. $z \in R^r$ is the

reduced unknown temperature state vector obtained through the state projection equation:

$$T \approx V \cdot z$$

$$(7)$$

By using the MOR methodology, the temperature distribution result of the full forearm model is approximated by the reduced model and the computational time is speeded up. Furthermore, according to equation (7), the full-scale unknow temperature state vector of the forearm model could be approximated by the multiplication of projection matrix and reduced state vector. This approximated full-scale temperature state vector could be further used as the temperature boundary conditions for detailed TEG submodel.

SIMULATION RESULTS

The thermal simulation of the human forearm model contains two steps. Firstly, a steady state thermal simulation is processed and its result is further used as an initial state for the transient thermal simulation in the second step, where the influence of the film coefficient in the convection boundary condition is investigated. Film coefficient 20W/m²K is set in the steady thermal simulation and changed to 5 W/m²K in the transient thermal simulation. According to the standards from European Pharmacopoeia, the room temperature is defined from 15 to 25°C. In our simulations, we selected the ambient temperature as constant at 15°C. "Convectoin-type" blood perfusion and constant metabolic heat generation rates are applied in the muscle, fat and skin layers. Before applying the submodeling technique, the representative TEG and detailed TEG models are placed in the forearm model and the temperature distribution results are compared (see Figure 6).
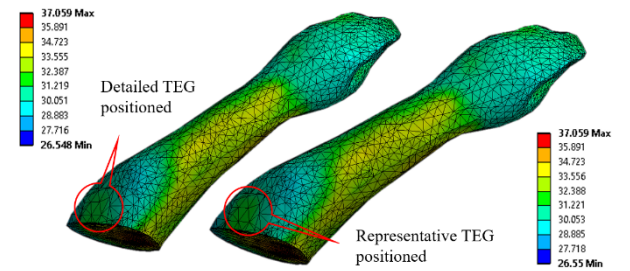

Figure 6: Comparison of the temperature results on the forearm model with detailed and representative TEG

The temperature relative error between the representative and detailed TEG positioned human forearm models are shown in Figure 7. It is observed that the maximum temperature relative error between the nodes of the forearm tissue model is 2%, which means that the temperature distribution result on the forearm model will not be influenced too much by the representative TEG. It is further shown that the temperature results from the representative TEG positioned forearm model could be

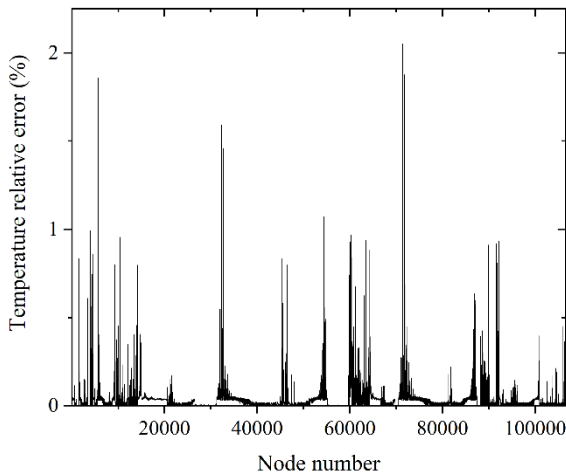used as the temperature boundary conditions for the detailed TEG submodel.

Figure 7: Temperature relative error between the forearm models with representative and detailed TEG (temperature results in TEG not included, total 106,550 DoF in the forearm tissue model without TEG)

In the next, the MOR algorithm is applied on the representative TEG positioned forearm model through the software ModelReduction inside ANSYS. The temperature results from the full and reduced models are compared (see Figure 8).
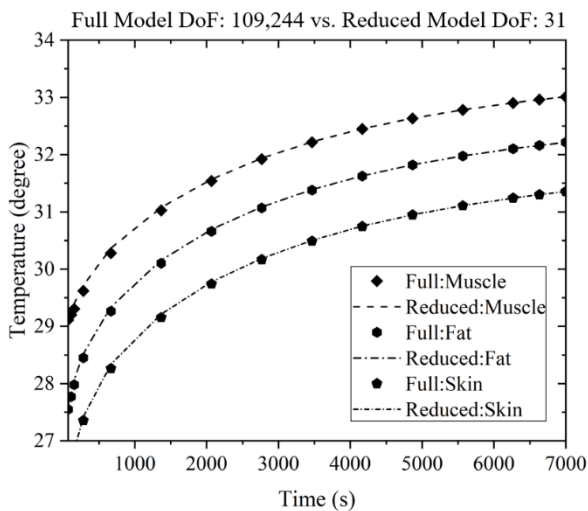

Figure 8: Temperature comparison between the full FE model with 109,244 DoF and reduced model with 31 DoF of the forearm model at selected nodes in muscle, fat and skin skin layers

The relative error between the full and reduced models are calculated (see Figure 9). Maximum relative errors in muscle, fat and skin layers are 0.33%, 0.3% and 0.27%, respectively. This shows that the reduced model is accurate enough for giving the temperature distribution result of the forearm model.
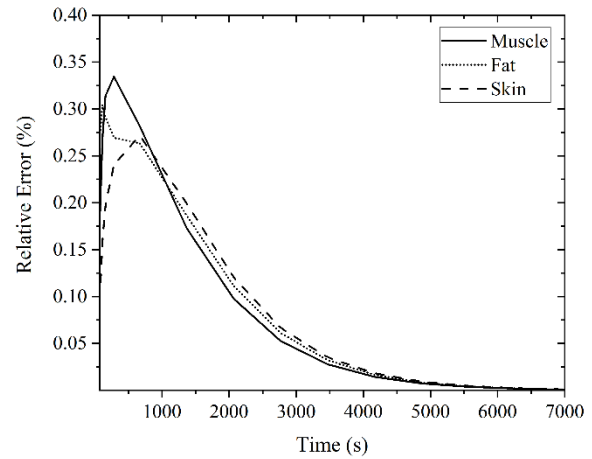

Figure 9: Relative error between the full-scale and reduced-order model at selected nodes in muscle, fat and skin layers

Based on the accurate reduced forearm thermal model, the full-scale temperature state vector is obtained through the projection equation (7). The distribution temperature results are further used as the temperature boundary conditions for the detailed TEG submodel. The detailed TEG is surrounded by a small amount of tissue, where the resulting temperature from the full-scale forearm model is applied (see Figure 10).
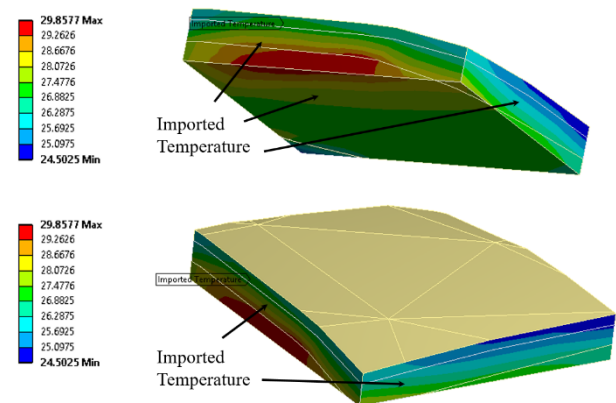

Figure 10: Applying resulting temperature from the full-scale forearm model as the temperature boundary conditions in the tissue surrounded detailed TEG

In this submodel, except the temperature boundary condtions, the convection effect at the skin surface, "convection-type" blood perfusion and metabolic heat generation rates in muscle, fat, skin layers are all applied. Through the simulation of the submodel, the temperature results on the detailed TEG will then be obtained and they could be further used to analyze the performance of TEG for the optimization design. The temperature results on the detailed TEG are compared between the submodeling and original full-scale model simulations (see Figure 11). The temperature relative errors on each node in the detailed TEG are calculated (see Figure 12). The maximum temperature relative error between the nodes

of the detailed TEG models is 8.01% and the average relative error is 1.94%, which shows that the temperature simulation results of the detailed TEG from the submodel is accurate enough.
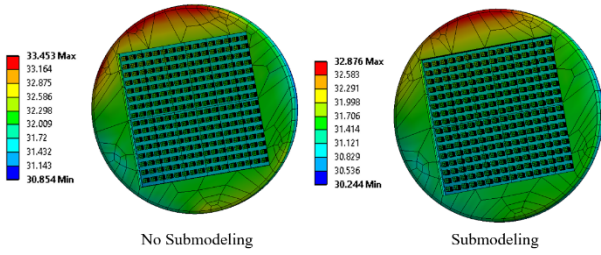

No Submodeling   Submodeling

Figure 11: Copmrison of the temperature results on the detailed TEG models. Left: Obtained result without submodeling technique; Right: Obtained result with submodeling technique
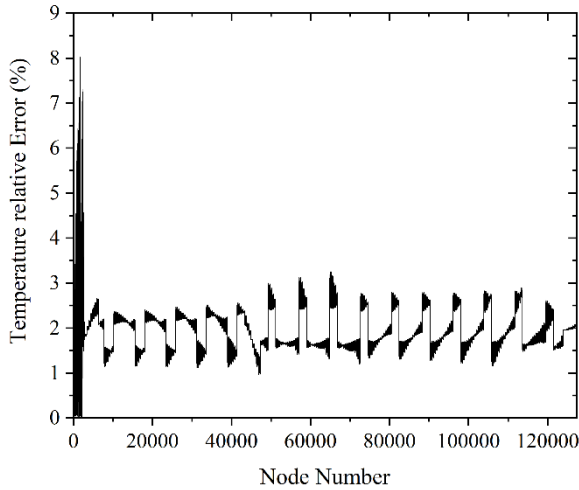

Figure 12: Temperature relative error between the detailed TEG models (total 127,307 DoF)

With submodeling technique, only the modifications and simulations in the submodel are required and no need for the re-computation of full thermal forearm model. The efficiency of the optimization process could be improved. The computational time for the whole MOR and submodeling process is shown in Table 3. The computational time used for the simulation of the detailed TEG in the complete forearm model is 1292.7s, which is 2.43 times longer than the simulation in submodel (557s). In addition, the steps of MOR and reprojection of full-scale temperature result in forearm model are required to be processed only once. This means the simulation time for the modified detialed TEG in the submodel is only 129.2s. It is 10 times faster than the simulation of the detailed TEG in the complete forarm model.

CONCLUSION AND OUTLOOK

In this paper, we present a combination of MOR and submodeling technique for the design optimization of a TEG embedded in human forearm tissue model. This approach speeds up the computational time for seeking the temperature distribution results on the TEG. Only the simulation of the TEG in a relatively small submodel is required. In the future, the TEG could be positioned in a complete human body model to find optimal performance. In addition, a multiphysics domain simulation is purposed based on the submodel and more complicated heat transfer effects, such as radiation and sweating, would be considered.

Table 3: Computational time comparison between the simulations of the detailed TEG in submodeled and complete forearm model (On Intel® CORE™ i5-7600 CPU@3.5GHz, 32GB RAM).

Computational Time	Simulation of detailed TEG in submodel	Simulation of detailed TEG in complete model
MOR	54.69s	
Reprojection	373.11s	
Submodeling	129.2s	
Total	557s	1292.7s

REFERENCES

Amar, A.B., A.B. Kouki, and H. Cao. 2015. "Power Approaches for Implantable Medical Devices". In *Sensors 2015*, 15, 28889-28914.

Antoulas, A.C. 2005. "Approximation of Large-scale Dynamical Systems" In *Society for Industrial and Applied Mathematics*.

Becthold, T., G. Schrag and L.H. Feng. 2013. "System-level Modeling of MEMS". Wiley-VCH Verlag GmbH & Co. KGaA.

Freund, R.W. 2000. "Krylov-Subspace Methods for Reduced-Order Modeling in Circuit Simulation". In *Journal of Computational and Applied Mathematics*, 123, 395-421.

Jadhav, O.S., C.D. Yuan, D. Hohlfeld and T. Bechtold. 2017. "Design of a thermoelectric generator for electrical active implants". In *MikroSystemTechnik Kongress 2017*, Germany, München.

Pennes, H.H. 1948. "Analysis of Tissue and Arterial Blood Temperatures in the Resting Human Forearm". In *Journal of Applied Physiology*, 1(2), 93-122.

Rudnyi, E.B. and J.G. Korvink. 2006. "Model Order Reduction for Large Scale Engineering Models Developed in ANSYS". In *Applied Parallel Computing*, 3732, 349-356.

Verma, U. 2018. "Modeling and Simulation of Bioheat Powered Subcutaneous Thermoelectric Generator". In *Proceedings of European Council for Modeling and Simulation 2018*, Germany, Wilhelmshaven.

Yang, Y., X.J. Wie and J. Liu. 2007. "Suitabiity of a Thermoelectric Power Generator for Implantable Medical Electronic Devices". In *Journal of Physics D: Applied Physics*, 40, 5790-5800.

Yalkoti, S.G. 2017. "Characterization of Thermoelectric Energy Conversion for Implantable Medical Devices". Master Thesis. Department of Computer Science and Electrical Engineering, University of Rostock, Germany.